

# The effect of glass-ceramic spray deposition on the bond strength of zirconia

Ting Xu<sup>a,b,c,d</sup>, Yuzhen Zhan<sup>a</sup>, Hang Chen<sup>a</sup>, Xuelu Tong<sup>a,b,c,d,\*</sup>, Xiaonan Zhang<sup>a,b,c,d,\*</sup>

<sup>a</sup> College of Stomatology, Chongqing Medical University, Chongqing 400016 China

<sup>b</sup> Chongqing Key Laboratory of Oral Diseases, Chongqing 401147 China

<sup>c</sup> Chongqing Municipal Key Laboratory of Oral Biomedical Engineering of Higher Education, Chongqing 401147 China

<sup>d</sup> Chongqing Municipal Health Commission Key Laboratory of Oral Biomedical Engineering, Chongqing 401147 China

\*Corresponding authors, e-mail: 500133@hospital.cqmu.edu.cn, 500793@hospital.cqmu.edu.cn

Received 15 May 2025, Accepted 18 Mar 2026

Available online 5 May 2026

**ABSTRACT:** Glass-Ceramic Spray Deposition (GCSD) is a novel technology that modifies zirconia surfaces by depositing a lithium disilicate glass layer. This study investigates the effect of GCSD on the shear bond strength (SBS) of zirconia compared to conventional bonding methods. Zirconia blocks were divided into three groups: Z (Z-Prime Plus), S (Single Bond Universal), and L (GCSD + LiSi Connect). Specimens were subdivided into 24 h water storage (unaged) and 5000 thermal cycling (aged) groups ( $n = 10$ ). SBS was tested, and fracture modes were analyzed. Surface morphology was examined via SEM. In the unaged condition, the L group exhibited the highest SBS ( $33.63 \pm 1.25$  MPa), which was significantly higher than that of Z group ( $31.15 \pm 2.26$  MPa) and S group ( $30.47 \pm 2.57$  MPa) ( $p < 0.05$ ). After aging, SBS significantly decreased in all groups ( $p < 0.05$ ). Although the L group maintained the highest mean value ( $28.87 \pm 1.94$  MPa) compared to S group ( $26.92 \pm 2.68$  MPa) and Z group ( $26.72 \pm 2.70$  MPa), no statistically significant differences were observed among the groups in the aged condition ( $p > 0.05$ ). GCSD surface modification achieved superior initial bond strength compared to 10-methacryloyloxydecyl dihydrogen phosphate (MDP)-based primers. Although bond strength decreased after aging, it remained at a level comparable to the control groups. Thus, GCSD presents a viable alternative for clinical zirconia bonding.

**KEYWORDS:** zirconia, lithium disilicate coating, bonding agent, shear strength, long-term stability

## INTRODUCTION

Zirconia ceramics have become a mainstream material in dental restorations due to their excellent mechanical properties and biocompatibility. However, the chemically inert surface of zirconia poses challenges in achieving sufficient bond strength, which remains a critical clinical issue [1,2]. Traditional methods such as sandblasting combined with 10-methacryloyloxydecyl dihydrogen phosphate (MDP)-based primers (e.g., Z-Prime Plus) or universal adhesives (e.g., Single Bond Universal) enhance initial bond strength through micromechanical interlocking and chemical bonding, yet their long-term stability is significantly compromised by interfacial hydrolysis and thermal stress [3–5]. Recently, glass-ceramic spray deposition (GCSD) technology, which involves sintering a lithium disilicate glass layer onto zirconia surfaces followed by hydrofluoric acid (HF) etching and silanization, has emerged as a novel approach for zirconia surface modification [6,7]. While Kang et al [8] demonstrated that GCSD combined with 90 s HF etching achieved bond strength comparable to lithium disilicate glass ceramics, the post-thermocycling strength decreased by approximately 20%. Thammajaruk et al [9] further attributed this durability limitation to hydrolysis of the glass phase within the coating. Alternative techniques such as

plasma treatment [10] and laser texturing [11] improve wettability but face practical constraints due to operational complexity and cost. The present study evaluates a GCSD protocol with a shortened HF etching time (45 s) and directly compares its long-term bond stability with both an MDP-containing primer and a universal adhesive under identical aging conditions.

## MATERIALS AND METHODS

### Sample preparation

Seventy-two high-purity zirconia ceramic blocks ( $8 \times 8 \times 2$  mm, TT-GT, UPCERA, China) were prepared. The samples were polished sequentially with 400-, 600-, 800-, and 1000-grit silicon carbide paper under water cooling, ultrasonically cleaned in ethanol for 6 min, and dried with clean airflow.

### Experimental grouping

A total of 72 zirconia specimens were randomly divided into three groups ( $n = 24$ ):

- Z group: treated with Z-Prime™ Plus (Bisco, USA).
- S group: treated with Single Bond Universal (3M, USA).
- L group: treated with Biomic™ LiSi Connect (Aidite, China).

Within each group, specimens were allocated as follows:

1. Surface characterization ( $n = 4$ ): four specimens were randomly selected for surface morphology observation (SEM) and elemental analysis (EDS) to evaluate the surface texture and composition after treatment.
2. Shear bond strength test ( $n = 20$ ): the remaining specimens were subdivided into two subgroups ( $n = 10$ ) for mechanical testing:
  - Unaged subgroup: stored in distilled water at 37 °C for 24 h.
  - Aged subgroup: subjected to 5000 thermal cycles between 5 °C and 55 °C, with a dwell time of 30 s and a transfer time of 5 s.

The sample size of 10 specimens per subgroup for shear bond strength testing was determined with reference to previous *in vitro* studies on zirconia-resin bonding that reported standard deviations of approximately a few megapascals (MPa) and considered differences of about 5 MPa or more to be clinically relevant, which commonly adopted 8–12 specimens per group for shear bond testing [12, 13]. Under these conditions, a priori power analysis using G\*Power 3.1 indicated that 10 specimens per subgroup were sufficient to provide at least 80% statistical power at a significance level of 0.05 for detecting meaningful differences in bond strength.

### Surface treatment

Z group: sandblasted with 50- $\mu\text{m}$   $\text{Al}_2\text{O}_3$  particles (29–36 psi, 10 mm distance), cleaned ultrasonically, and coated with Z-Prime Plus.

S group: sandblasted similarly, then coated with Single Bond Universal, and light-cured for 10 s.

L group: sprayed with LiSi Connect, sintered in a furnace (Program: 450 °C to 900 °C, 80 °C/min, hold for 1.5 min), etched with 9.5% HF (45 s), cleaned, silanized, and coated with porcelain bonding resin.

### Bonding procedure

A cylindrical glass mold ( $\phi = 3$  mm,  $h = 3$  mm) was placed on the treated zirconia surface. Duo-Link resin cement (Bisco, USA) was injected into the mold, light-cured for 20 s, and stored in 37 °C water for 24 h.

### Thermal cycling

A randomly selected half of the samples underwent 5000 thermal cycles between 5 °C and 55 °C using a thermal cycling machine (TC-501F (III), WeiEr, China), while the remaining half served as non-thermocycled controls.

### Shear bond strength test

Shear force was applied at 0.5 mm/min using a universal testing machine (C43.104, MTS, China). Bond

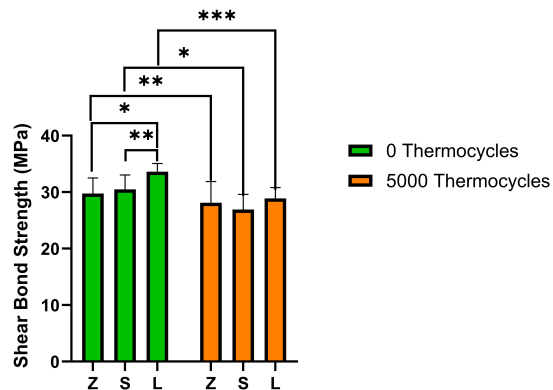


Fig. 1 Impact of different surface treatment methods on the shear bond strength of zirconia: comparison before and after thermocycling.

strength (MPa) was calculated as force (N) divided by bonded area ( $\text{mm}^2$ ).

### Fracture mode analysis

Classification based on failure mechanism (adhesive/cohesive/mixed):

Adhesive failure: bond failure at the glass-ceramic or zirconia surface.

Cohesive failure: failure within the resin cement.

Mixed failure: combined adhesive and cohesive failure.

### Surface morphology

Surface morphology was observed using SEM (SU8010, Hitachi, Japan) at 5 kV.

### Statistical analysis

Shear bond strength data were analyzed using two-way ANOVA and simple effect analysis (SPSS 23.0). A  $p$ -value  $< 0.05$  was considered statistically significant. Statistical analysis was conducted to determine the influence of different surface treatments and aging conditions on bond strength, providing insights into the most effective approaches for enhancing long-term adhesion between zirconia and resin cements.

## RESULTS

### Shear bond strength

The shear bond strength results are presented in Fig. 1. In the unaged condition, all three groups exhibited high bond strength ranging from 30.47 to 33.63 MPa. The L group achieved the highest value ( $33.63 \pm 1.25$  MPa), followed by the Z group ( $31.15 \pm 2.26$  MPa) and S group ( $30.47 \pm 2.57$  MPa). One-way ANOVA revealed statistically significant differences among the three groups ( $p < 0.01$ ). Further

**Table 1** Distribution of fracture modes in different groups before and after aging.

Group	Mode		
	A	M	C
S-Unaged	1	9	0
Z-Unaged	0	10	0
L-Unaged	2	8	0
S-Aged	1	9	0
Z-Aged	0	10	0
L-Aged	2	8	0

post-hoc analysis indicated that the L group had significantly higher bond strength compared to the Z and S groups, while no significant difference was found between the Z and S groups.

After 5000 thermal cycles, the bond strength significantly decreased in all groups compared to the unaged baseline ( $p < 0.05$ ). The L group decreased to  $28.87 \pm 1.94$  MPa (approximately 14.2% reduction), the Z group to  $26.72 \pm 2.70$  MPa (14.2% reduction), and the S group to  $26.92 \pm 2.68$  MPa (11.7% reduction). Although the L group maintained the highest mean value numerically, statistical analysis showed no significant differences in bond strength among the three groups after aging ( $p > 0.05$ ).

### Fracture mode analysis

#### Fracture mechanism classification

The results indicated that in the unaged condition, all groups (S, Z, and L) predominantly exhibited mixed failure (Mixed, M), with some specimens in the S and L groups showing pure adhesive interfacial failure (Adhesive, A). After aging, all groups still mainly exhibited mixed failure, with some specimens in the S and L groups showing pure adhesive failure (Adhesive, A) (Table 1).

#### Macroscopic and microscopic morphology of the fracture surfaces

The results showed that both before and after aging, the S and Z groups exhibited similar fracture morphologies, mainly characterized by mixed failure or extensive resin detachment, whereas in the L group, distinct resin remnants were observable on parts of the fracture surface (Fig. 2).

### Surface morphology examination

#### Surface morphology after sandblasting and acid etching

The results revealed that the zirconia surfaces of the S and Z groups, after sandblasting, exhibited a uniformly roughened structure with fine particles distributed on the surface (Fig. 3A,B). In contrast, the L group, after acid etching, displayed a distinct exposed crystal structure, and the acid etching of the glass-ceramic

coating resulted in more micro-pits and roughened areas (Fig. 3C,D).

#### Surface morphology of the L group before and after aging

The results showed that in the unaged condition, the zirconia surface, after being sprayed with a glass-ceramic layer, exhibited a uniformly distributed micro-crystalline structure (Fig. 4A,B). After 5000 thermal cycles, minor pores or cracks appeared locally at the zirconia and resin interface, but the overall structure remained relatively intact (Fig. 4C,D).

#### Elemental analysis of the sandblasted surface

The analysis results indicate that the primary components on the surface are zirconia (Zr and O), with zirconium and oxygen accounting for 55.96% and 31.68% by weight, respectively, which is consistent with the fundamental characteristics of the zirconia ceramic matrix. Additionally, trace amounts of C (8.26%), Al (1.30%), and Y (2.80%) were detected (Table 2 and Fig. 5).

### DISCUSSION

The results of this study demonstrated that the GCSD technology effectively enhances the shear bond strength of zirconia. The initial bond strength of the GCSD group (L group:  $33.63 \pm 1.25$  MPa) was significantly higher than that of the Z-Prime Plus group (Z group:  $31.15 \pm 2.26$  MPa) and Single Bond Universal group (S group:  $30.47 \pm 2.57$  MPa) ( $p < 0.05$ ). These values exceed the minimum threshold considered clinically acceptable for ceramic bonding [14, 15]. The superior performance of the L group aligns with previous studies on glass-ceramic coatings, confirming that the lithium disilicate layer provides a dual-retention mechanism: micromechanical interlocking via surface roughness and chemical bonding through silane coupling agents [9, 16].

A critical optimization in this study was the hydrofluoric acid (HF) etching duration. While some established protocols recommend extended etching times (e.g., 90 s) [17], this study optimized the duration to 45 s. Our pilot experiments indicated that for the specific coating thickness achieved in our process, a 90 s exposure caused excessive dissolution of the glass phase, leading to substrate exposure and potential coating detachment. This observation is supported by literature indicating that over-etching can weaken the ceramic network and reduce the effective surface area for bonding [18, 19]. The SEM images confirmed that 45 s was sufficient to create a retentive crystalline topography without compromising structural integrity, highlighting the importance of tailoring etching protocols to the specific density and thickness of the coating [20, 21].

Long-term stability remains the primary challenge for zirconia-resin interfaces. After 5000 thermal

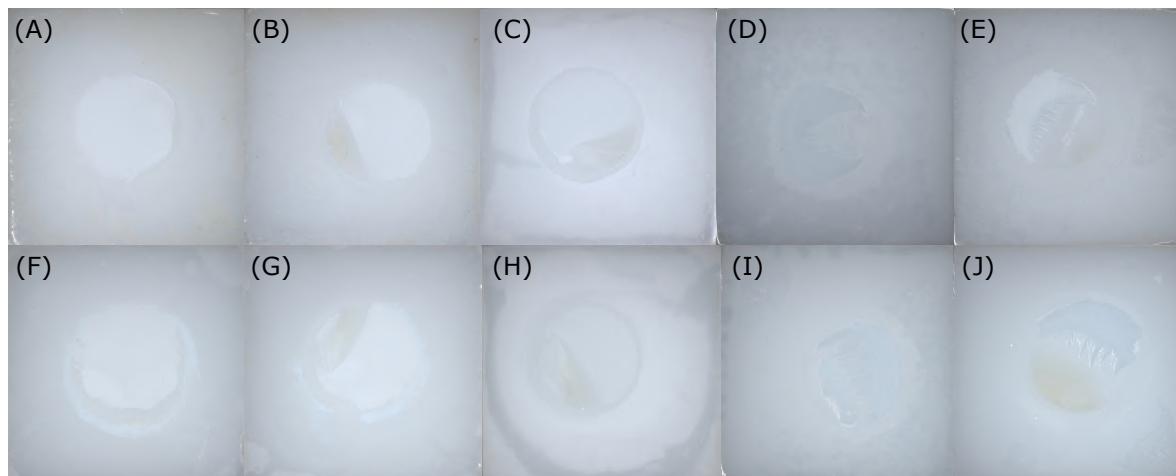


**Fig. 2** Fracture mode analysis of different groups before and after aging. A: Unaged S group (Adhesive failure); B: Unaged S group (Mixed failure); C: Unaged Z group (Mixed failure); D: Unaged L group (Adhesive failure); E: Unaged L group (Mixed failure); F: Aged S group (Adhesive failure); G: Aged S group (Mixed failure); H: Aged Z group (Mixed failure); I: Aged L group (Adhesive failure); J: Aged L group (Mixed failure).

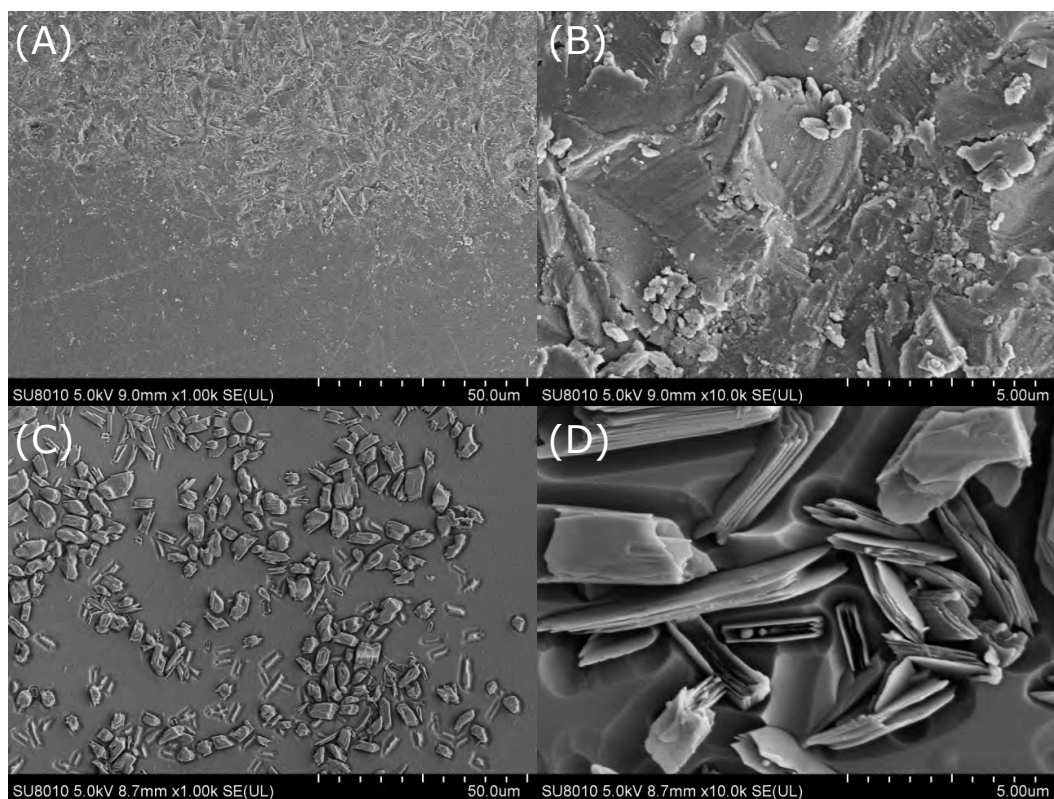


**Fig. 3** Surface morphology of zirconia and resin after sandblasting and acid etching. A: Z and S groups - Sandblasting treatment: SEM image of the zirconia surface after sandblasting, showing a rough surface texture with scattered small particles at 1,000 $\times$  magnification. B: Z and S groups - Sandblasting treatment (higher magnification): higher magnification of the sandblasted zirconia surface, showing more defined roughness and particle distribution at 10,000 $\times$  magnification. C: L group - Acid etching treatment: SEM image of the zirconia surface after acid etching, showing a more textured surface with exposed crystalline structures at 1,000 $\times$  magnification. D: L group - Acid etching treatment (higher magnification): higher magnification image showing distinct crystalline structures and roughened surface after acid etching at 10,000 $\times$  magnification.

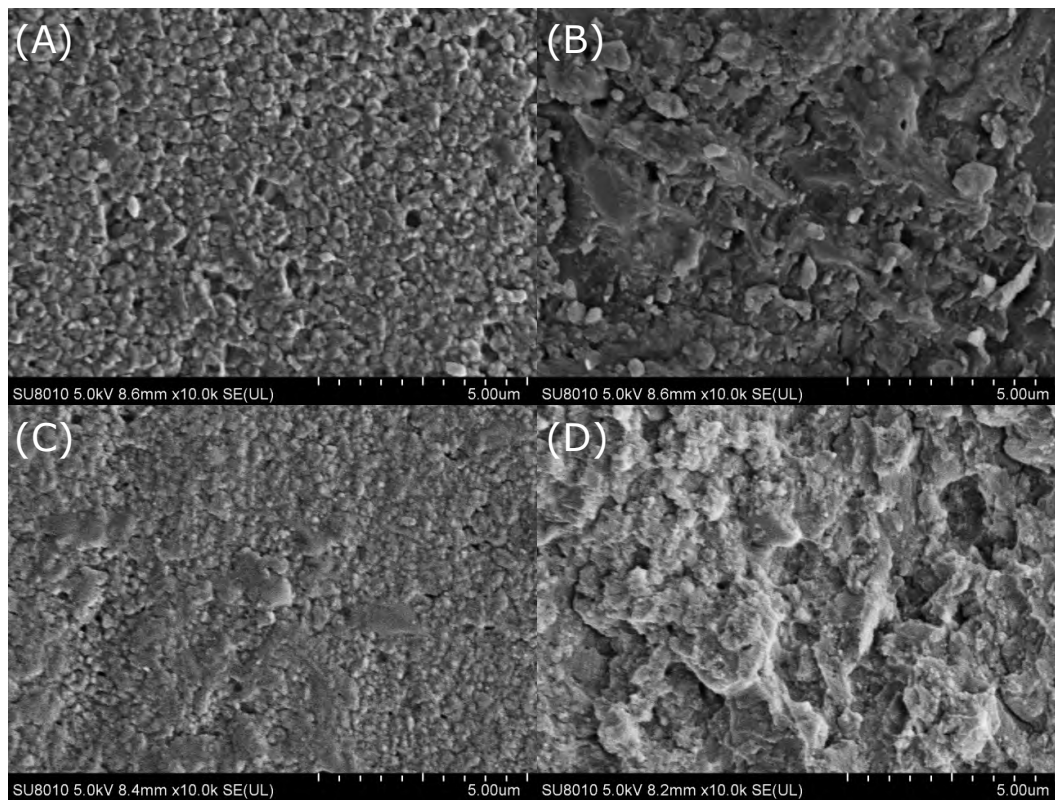


**Fig. 4** Scanning Electron Microscopy (SEM) images of L group surface morphology before and after aging. A: Unaged zirconia surface - SEM image showing the surface morphology of zirconia after shearing, magnified at 10,000×; B: Unaged resin surface - SEM image showing the resin surface morphology after shearing, magnified at 10,000×; C: Aged zirconia surface - SEM image showing the zirconia surface morphology after thermal cycling, magnified at 10,000×; D: Aged resin surface - SEM image showing the resin surface morphology after thermal cycling, magnified at 10,000×.

**Table 2** Elemental analysis of the sandblasted surface.

Element	Line type	Apparent concentration	k ratio	Wt %	Wt % sigma	Standard label	Factory standard
C	K series	2.07	0.021	8.26	0.45	C Vit	Yes
O	K series	37.46	0.126	31.68	0.35	SiO <sub>2</sub>	Yes
Al	K series	2.49	0.018	1.30	0.05	Al <sub>2</sub> O <sub>3</sub>	Yes
Y	L series	4.40	0.044	2.80	0.30	Y	Yes
Zr	L series	89.36	0.894	55.96	0.44	Zr	Yes

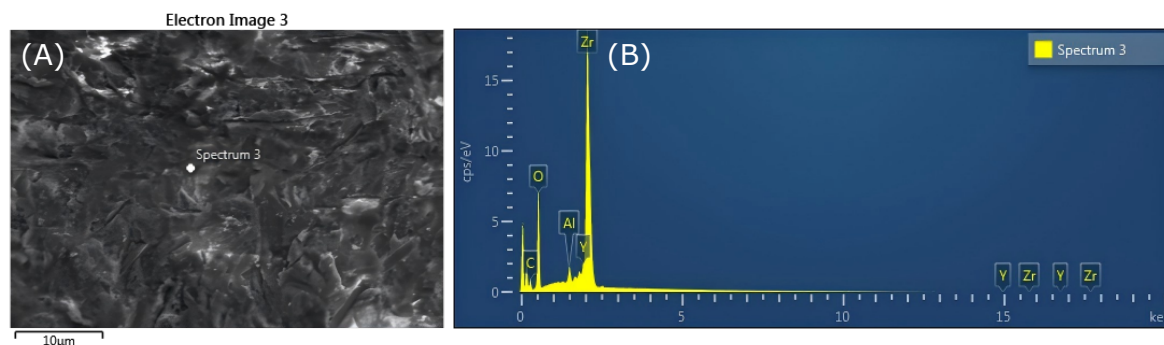


**Fig. 5** Surface morphology and elemental distribution analysis of sandblasted zirconia ceramics. A: SEM image of the zirconia surface after sandblasting; B: EDS spectrum of the corresponding area.

cycles, bond strength significantly decreased in all groups ( $p < 0.05$ ). Specifically, the L group exhibited a reduction of approximately 14.2% (decreasing to  $28.87 \pm 1.94$  MPa). Notably, this reduction rate is lower than the decrease reported in similar glass-ceramic coating studies, which often show reductions exceeding 20% after aging [9, 16]. The improved stability in this study may be attributed to the optimized etching protocol preserving a more stable glass matrix. However, microcracks were still observed in the L group after aging, consistent with the theory of thermal expansion mismatch between the glass coating and the zirconia substrate, which can accelerate interfacial fatigue [16].

Fracture mode analysis revealed that the L group predominantly exhibited mixed failures with resin remnants on the zirconia surface. From a clinical perspective, a mixed failure mode indicates that the adhesive interface strength is comparable to or exceeds the cohesive strength of the resin cement [22]. In contrast, the adhesive failures observed in the control groups suggest a weaker link at the interface, which poses a higher risk of restoration debonding under occlusal forces. The ability of the GCSD surface to maintain resin retention after aging underscores its potential to reduce the risk of catastrophic restoration detachment in clinical scenarios.

This study has limitations that warrant further investigation. The sample size ( $n = 10$ ) provided sufficient statistical power for this *in vitro* setup, but larger sample sizes are recommended for verifying clinical consistency. Additionally, while thermal cycling simulates aging, the oral environment also involves mechanical fatigue and pH fluctuations [23, 24]. Future research should focus on optimizing the sintering parameters to further reduce thermal mismatch and exploring the fatigue resistance of GCSD-treated zirconia under dynamic loading conditions [25, 26]. Moreover, the SEM observations in this study were qualitative; profilometric or three-dimensional roughness parameters (e.g., Ra, Rz) and quantitative porosity metrics were not measured, which limits the ability to directly correlate surface topography with the observed differences in bond strength.

## CONCLUSION

Within the limitations of this *in vitro* study, application of a lithium disilicate glass-ceramic coating to zirconia by GCSD produced high initial shear bond strengths of 30.47–33.63 MPa and maintained values of 26.72–28.87 MPa after 5000 thermal cycles. The GCSD group showed higher bond strength than the MDP-containing primer and the universal adhesive before aging, with statistically significant differences ( $p < 0.01$ ), whereas after aging, the differences among the three groups were no longer statistically significant ( $p > 0.05$ ). Mixed failure modes with resin remnants on the zirconia surface predominated in all groups, indicating that

the adhesive interface strength approached the cohesive strength of the resin cement and may be clinically acceptable under the tested conditions. Nevertheless, all surface treatments exhibited a significant reduction in bond strength after aging, underscoring the need to further optimize GCSD parameters and evaluate its performance under combined thermal, mechanical, and chemical aging before definitive clinical recommendations can be made.

**Acknowledgements:** This work was financially supported by the National Natural Science Foundation of China (81700982) and the Chongqing Medical Reserve Talent Studio for Young People (ZQNYXGDRCGZS2019004).

## REFERENCES

1. Wang Y, Hui R, Gao L, Ma Y, Wu X, Meng Y, Hao Z (2022) Effect of surface treatments on bond durability of zirconia-reinforced lithium silicate ceramics: An *in vitro* study. *J Prosthet Dent* **128**, 1350.e1–1350.e10.
2. Duangphet S, Intatha U, Soykeabkaew N, Khongphinitbunjong K (2025) Comparative study on the flexural properties and hardness of a PMMA-based dental composite. *ScienceAsia* **51**, ID 2025082.
3. Kim SH, Oh KC, Moon HS (2024) Effects of surface-etching systems on the shear bond strength of dual-polymerized resin cement and zirconia. *Materials* **17**, 3096.
4. Brown T, Kee E, Xu X, Chapple A, Stamitole C, Armbruster PC, Ballard RW (2024) Shear bond strength of orthodontic brackets bonded to high-translucent dental zirconia with different surface treatments: An *in vitro* study. *Int Orthod* **22**, 100822.
5. Santos Silva MMMD, Boucault CHM, Steagall W, Hanashiro FS, Cardoso CAB, de Souza-Zaroni WC, Youssef MN, do Amaral SF (2024) Influence of different surface treatments on the bond strength of yttria-stabilized tetragonal zirconia ceramic. *Photobiomodul Photomed Laser Surg* **42**, 343–349.
6. Riesgo BVP, Rodrigues CS, do Nascimento LP, May LG (2023) Effect of hydrofluoric acid concentration and etching time on the adhesive and mechanical behavior of glass-ceramics: A systematic review and meta-analysis. *Int J Adhes Adhes* **121**, 103303.
7. Thammajaruk P, Buranadham S, Guazzato M, Wang Y (2021) Shear bond strength of composite cement to lithium-disilicate glass-coated zirconia versus alumina air-abraded zirconia. *J Adhes Dent* **23**, 267–275.
8. Kang CM, Lin DJ, Feng SW, Hung CY, Iwaguro S, Peng TY (2022) Innovation glass-ceramic spray deposition technology improving the adhesive performance for zirconium-based dental restorations. *Int J Mol Sci* **23**, 12783.
9. Thammajaruk P, Buranadham S, Prasansuttiporn T, Guazzato M (2023) Influence of a novel lithium disilicate coating on composite-zirconia bonding and bond characterization. *Int J Prosthodont* **36**, 172–180.
10. Jiang Y, Bao X, Yu Y, Zhang Y, Liu M, Meng F, Wang B, Chen J (2024) Effects of different plasma treatments on bonding properties of zirconia. *Heliyon* **10**, e32493.
11. Souza M, Raffaele-Esposito A, Carvalho O, Silva F, Özcan M, Henriques B (2023) Surface modification of zirconia

- or lithium disilicate-reinforced glass ceramic by laser texturing to increase the adhesion of prosthetic surfaces to resin cements: An integrative review. *Clin Oral Investig* **27**, 3331–3345.
12. Steiner R, Heiss-Kisielewsky I, Schwarz V, Schnabl D, Dumfahrt H, Laimer J, Steinmassl O, Steinmassl PA (2019) Zirconia primers improve the shear bond strength of dental zirconia. *J Prosthodont* **29**, 62–68.
  13. Pott PC, Stiesch M, Eisenburger M (2015) Influence of 10-MDP adhesive system on shear bond strength of zirconia-composite interfaces. *J Dent Mater Tech* **4**, 117–126.
  14. Dimitriadis K, Tulyaganov DU, Agathopoulos S (2024) Evaluation of bond strength between zirconia milled ceramic material and veneered dental porcelain. *Eur J Oral Sci* **132**, e12989.
  15. Khalil AA, Abdelaziz KM (2015) Bonding values of two contemporary ceramic inlay materials to dentin following simulated aging. *J Adv Prosthodont* **7**, 446–453.
  16. Shen D, Wang H, Shi Y, Su Z, Hannig M, Fu B (2023) The effect of surface treatments on zirconia bond strength and durability. *J Funct Biomater* **14**, 89.
  17. You GE, Lim MJ, Min KS, Yu MK, Lee KW (2024) Surface property changes observed in zirconia during etching with high-concentration hydrofluoric acid over various immersion times. *Dent Mater J* **43**, 52–57.
  18. Jin C, Wang J, Huang Y, Yu P, Xiong Y, Yu H, Gao S (2022) Effects of hydrofluoric acid concentration and etching time on the bond strength to ceramic-coated zirconia. *J Adhes Dent* **24**, 125–136.
  19. Ramakrishnaiah R, Alkheraif AA, Divakar DD, Matinlinna JP, Vallittu PK (2016) The effect of hydrofluoric acid etching duration on the surface micromorphology, roughness, and wettability of dental ceramics. *Int J Mol Sci* **17**, 822.
  20. Zhang X, Nie H, Lv J, Yuan S, Wang J, Cai K, Wu J, Zhang Q, et al (2024) Evaluation of zirconia surfaces and shear bond strength after acid-etching with ultrasonic vibration. *Mater Res Express* **11**, 025401.
  21. Seo SH, Kim JE, Nam NE, Moon HS (2022) Effect of air abrasion, acid etching, and aging on the shear bond strength with resin cement to 3Y-TZP zirconia. *J Mech Behav Biomed Mater* **134**, 105348.
  22. Wu X, Xie H, Meng H, Yang L, Chen B, Chen Y, Chen C (2019) Effect of tribochemical silica coating or multipurpose products on bonding performance of a CAD/CAM resin-based material. *J Mech Behav Biomed Mater* **90**, 417–425.
  23. Lima VP, Machado JB, Zhang Y, Loomans BAC, Moraes RR (2022) Laboratory methods to simulate the mechanical degradation of resin composite restorations. *Dent Mater* **38**, 214–229.
  24. Fadavi F, Mohammadi-Bassir M, Sarabi N, Rezvani MB, Jafari-Semnani S, Rastegar Moghaddam M, Labbaf H (2023) Effect of low-temperature degradation, pH-cycling and simulated tooth brushing on surface roughness, topography and polish retention of yttrium-stabilized tetragonal zirconia. *J Dent (Shiraz)* **24**, 293–304.
  25. Yan Y, Shu F, Chen H, Dun Z, Lv W, Zhang Z, Sun W, Liu M (2022) Reinforcement of bonding strength between dental Y-TZP and resin via nano-thin and conformal SiO<sub>2</sub> films by atomic layer deposition. *Adv Mater Interfaces* **10**, 2201910.
  26. Rodrigues MR, Grangeiro MTV, Rossi NR, de Carvalho Ramos N, de Carvalho RF, Kimpara ET, Tribst JPM, de Arruda Paes Junior TJ (2022) Influence of optional crystallization firing on the adhesion of zirconia-reinforced lithium silicate before and after aging. *Coatings* **12**, 1904.